



Energy efficient air to air heat pump operating with R-1234yf

Sorina Mortada, Denis Clodic, Christine Arzano-Daurelle

► To cite this version:

Sorina Mortada, Denis Clodic, Christine Arzano-Daurelle. Energy efficient air to air heat pump operating with R-1234yf. 10th International Energy Agency Heat Pump Conference 2011 - HPC 2011, May 2011, Tokyo, Japan. 8 p. hal-00770147

HAL Id: hal-00770147

<https://hal-mines-paristech.archives-ouvertes.fr/hal-00770147>

Submitted on 7 Jan 2013

HAL is a multi-disciplinary open access archive for the deposit and dissemination of scientific research documents, whether they are published or not. The documents may come from teaching and research institutions in France or abroad, or from public or private research centers.

L'archive ouverte pluridisciplinaire **HAL**, est destinée au dépôt et à la diffusion de documents scientifiques de niveau recherche, publiés ou non, émanant des établissements d'enseignement et de recherche français ou étrangers, des laboratoires publics ou privés.

ENERGY EFFICIENT AIR TO AIR HEAT PUMP OPERATING WITH R-1234yf

Sorina Mortada, Ph.D. student, Center for Energy and Processes, MINES ParisTech, Paris, France

Denis Clodic, Professor, Center for Energy and Processes, MINES ParisTech, Paris, France

Christine Arzano-Daurelle, Research Engineer, EnerBAT, EDF R&D, Moret sur Loing, France

Abstract: Significant improvements in energy performance of air-to-air heat pumps are the major reason of their introduction in the late '90s for heating buildings in Japan and several European countries. They are installed in multi-dwelling units and in individual houses. Some of them are using variable speed compressors. European existing air-to-air heat pumps are not adapted for the low-energy building requirements. Their heating capacity is relatively higher than the heating demand and their energy efficiency is not sufficient.

This paper presents a low-capacity heating system: a mini-heat pump (MHP). The MHP consists of mini-channel heat exchangers for the condenser and evaporator. In order to improve the overall energy efficiency, a recovery air-to-air heat exchanger (RHX) fulfills a significant part of a passive house heating demand.

A first prototype of the MHP is realized and series of tests are presented in this paper with two refrigerants: R-134a and R-1234yf.

Keywords: Air to air heat pump, R-1234yf, energy efficiency

1. INTRODUCTION

European countries have made commitments to improve energy efficiency of 20% and to lower greenhouse-gas emissions also of 20% at the horizon of 2020. To reduce energy consumption standards are reinforced in the building sector because it represents 47% of the energy consumption in France (Figure 1). A low-energy consumption building, as defined in the French RT 2012, is a new building that consumes less than 50 kWh.m⁻².yr⁻¹ of primary energy (for heating, cooling, domestic hot water, ventilation, and lighting).

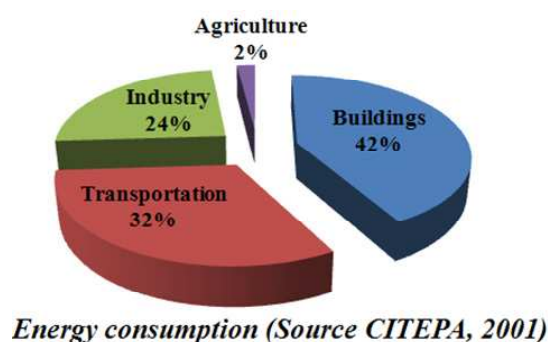


Figure 1: Sectors of energy consumption in France

The MHP prototype design has been performed taking into account an energy need of 15 kWh.m⁻².yr⁻¹ of primary energy for heating only; the consequence is a maximum heating capacity of 2 kW for an outdoor temperature of -7 °C. The MHP is a part of the air handling system of an individual house and includes three heat exchangers. Condenser and evaporator are mini-channel heat exchangers (MCHE) combining high heat transfer coefficients and low refrigerant charge reduction. The third air-to-air heat exchanger recovers heat from exhaust air and transfers it to the fresh air intake.

2 SYSTEM DESCRIPTION

A current air-to-air heat pump consists of extracted and fresh airflows blown into the condenser and the evaporator respectively in order to ensure the heating demand. In Europe, air-to-air heat pumps are usually split systems (Figure 2). The MHP uses a RHX allowing the heat exchange between the fresh air needed for the ventilation and the exhaust air. Both latent and sensible heats are transferred.

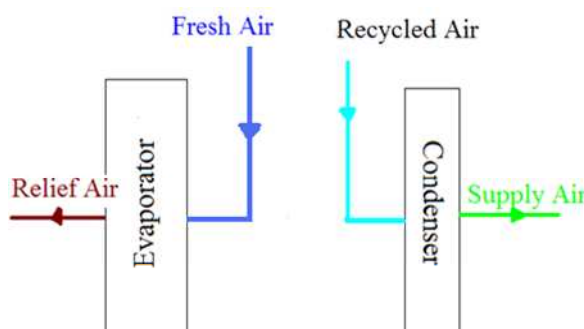


Figure 2: Schematic description of an air-to-air HP

The ventilation must be permanent as defined in the French building regulation. The minimum fresh airflow rate needed for ventilating a building is defined according to the building type and its occupancy. This airflow rate covers part the heating demand of low-energy building, the amount depends on the heat exchanger efficiency. This RHX can ensure up to 30% of the heating demand for 100% efficiency when the fresh air temperature exceeds 11°C. Figure 3 shows schematic diagram of the MHP.

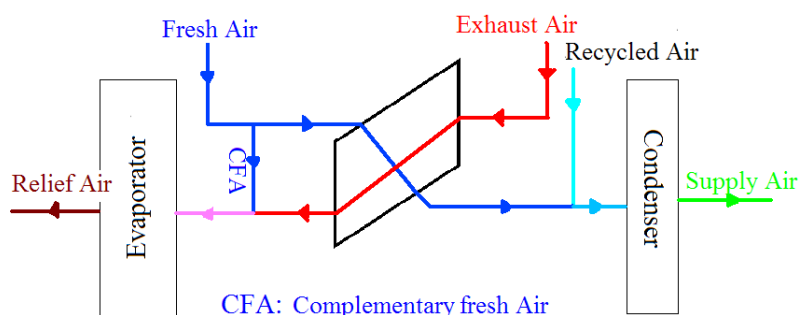


Figure 3: Schematic description of mini-heat pump (MHP)

To adapt to the heating demand along the heating season, variable-speed compressors and variable speed fans are chosen for the MHP prototype. The exhaust air leaving the RHX is mixed with complementary fresh airflow before passing on the evaporator. This complementary fresh air flow rate is controlled by a variable speed fan.

Micro-channel condenser and evaporator deliver a higher capacity of about 30% compared to the conventional fin-and-tube heat exchangers and lower pressure drop of about 33% (Mortada 2010). Besides, they are light and compact.

3 TEST BENCH

Figure 4 presents a layout of the test bench used to measure the MHP energy performances. Two small climatic rooms have been specifically designed and built for these tests. Due to the heat pump low capacity and the low range of airflow rates, measurements are delicate and require a precise metrology. These climatic rooms simulate air flows: from one room the air is exhausted and fresh air is blown in the other. These two rooms communicate via damper ensuring the pressure balance. The heating needs are simulated by a cooling capacity, which is delivered in those rooms by heat exchangers where a heat transfer fluid

(HTF) flows. Those cooling capacities are adjusted for each outdoor temperature. The MHP is designed to deliver the required heating demand.

Figure 4 shows a schematic lay-out of the connections between the MHP, the climatic rooms, and the measurement apparatuses.

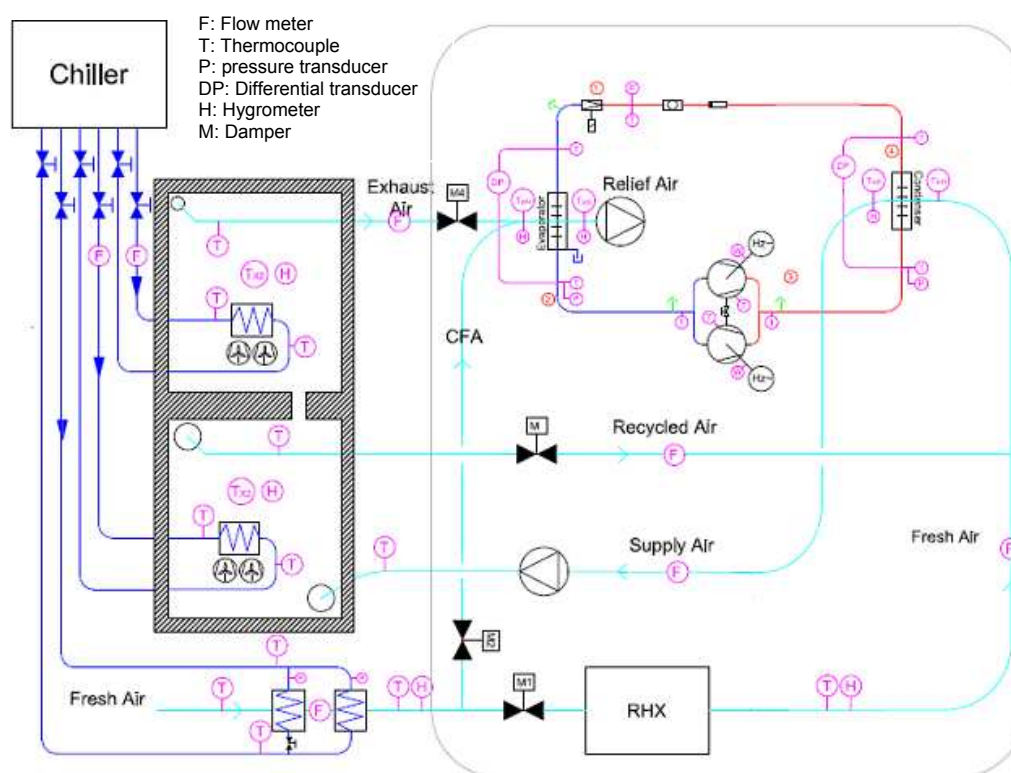


Figure 4: Schematic lay-out of the test bench

Air flow rate measurements are made by compensated orifice plates installed inside the ducts. Dry and wet bulb temperatures are measured for each air flow rate especially at the evaporator inlet and outlet. HTF flow rates are measured by electromagnetic flow-meters. The refrigerant loop measurements are using pressure transducers and thermocouples at the inlet and the outlet of each component. Speeds of compressors and fans are controlled via field point modules and their input powers are measured.

Table 1: Accuracy of the measurement apparatus

Apparatus	Accuracy
Pt100 class A	$\pm (0.15 + 0.002 T)$ where $ T $ = Temperature °C
Hygrometer	$\pm 0.8\%$ if $10^{\circ}\text{C} < T < 20^{\circ}\text{C}$ $\pm 1.3\%$ for other T
Air flow meter	$\pm 0.5\%$
Pressure Transducer	$\pm 0.15\%$
Multi-meters	$\pm 0.5\%$

Based on standard NF ENV 13005, uncertainty calculations were made. Type B is applied; this uncertainty calculation is based on the manufacturer declaration of its apparatus accuracy ($a=\pm\dots$).

The uncertainty Type B ($u(g_k)$) where g_k is the measured variable is calculated in Equation 1.

$$u(g_k) = \sqrt{\frac{(a_+ - a_-)^2}{12}} \quad (\text{Eq. 1})$$

If little information is provided by the manufacturer, the probability cannot be uniform throughout the interval. The standard advises to calculate the uncertainty using Equation 2:

$$u(g_k) = \frac{a}{\sqrt{12}} \quad (\text{Eq. 2})$$

An indirect measure is calculated from measured values. The overall uncertainty of g where g is the estimation of $G = f(x_1, x_2, x_3, \dots)$ is calculated by an appropriate mix of uncertainties ($u^2(x_k)$) for inputs x_k (Equation 3).

$$u_c^2(g) = \sum_{k=1}^N \left(\frac{\partial f}{\partial x_k} \right)^2 u^2(x_k) \quad (\text{Eq. 3})$$

The expanded uncertainty U is obtained by multiplying the combined standard uncertainty by a coverage factor k .

$$U(g) = k u_c(g) \quad (\text{Eq. 4})$$

k value is chosen based on known level of confidence required for the interval $[g + U; g - U]$. The standard suggests that by choosing $k = 2$, the interval has a confidence level of 95% and choosing $k = 3$ provides a confidence level of 99%. This method is used to calculate the uncertainty for the MHP tests.

4 RESULTS

The test procedure consists in:

- setting the outdoor temperature by adjusting the HTF flow rate
- adjusting the cooling load inside test rooms
- running the heat pump in order to maintain a room constant temperature (19°C)

Tests are run with R-134a and R-1234yf under the same conditions for different outdoor temperatures.

4.1 Climate rooms

Tests were first run in order to characterize the heat flow through the partition wall from the indoor-side to the outdoor-side compartment. Figure 5 shows the heat loss through the walls as a function of the DT ($T_{\text{outdoor}} - T_{\text{indoor}}$). In fact, the insulation thickness is 103 mm on all sides except the common surface between the two rooms where the thickness is 53 mm avoiding wall heat losses.

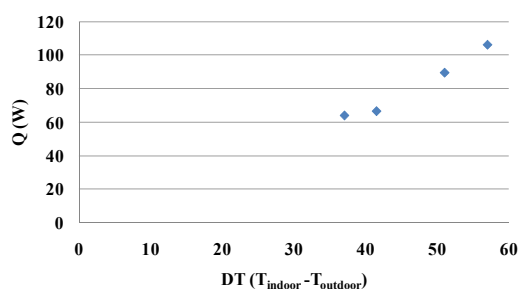


Figure 5: Heat loss through walls

4.2 Recovery heat exchanger

Heating demand is calculated using the building simulation software COMFIE. Three different French regions were simulated. The maximal heating demand is 2 kW for a 112-m² house in the Trappes region (mild oceanic climate). This heating demand is compared to the heating capacity recovered by the RHX.

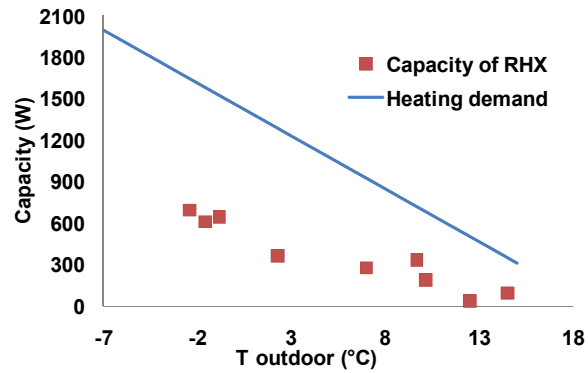


Figure 6: Heating demand and RHX as a function the outdoor temperature

Figure 7 shows the variation of the recovery heat exchanger effectiveness with the outdoor temperature. This effectiveness decreases with increasing the fresh air temperature.

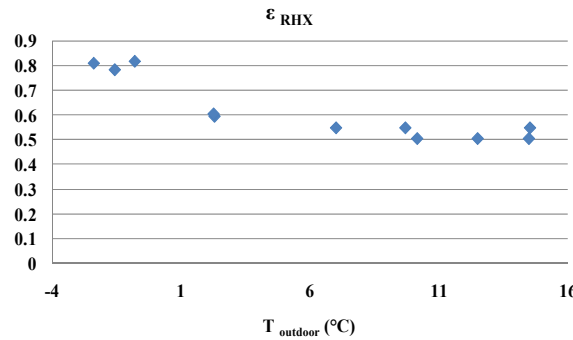


Figure 7: RHX efficiency as a function of the outdoor temperature

4.3 System

Compressors and fans are switched on when the RHX cannot ensure the heating demand. The coefficient of performance of MHP is defined by Equations 5 and 6 where Q_{loss} is the heat lost through the room walls.

$$COP_{Thermod y n a m i c} = \frac{Q_{Condenser} - Q_{loss}}{W_{Compressor}} \quad (\text{Eq. 5})$$

$$COP_{System_MHP} = \frac{Q_{Condenser} + Q_{RHX} - Q_{loss}}{W_{Compressors} + W_{sup plyfan}} \quad (\text{Eq. 6})$$

The control parameters are the airflow rate related to the fan speed and the air supply temperature related to a comfort temperature inside the house. The air supply temperature affects the condensation temperature: the higher the air supply temperature, the higher the condensing pressure and so the lower the COP.

Figure 8 shows the variation of the $COP_{thermodynamic}$ as a function of the outdoor temperature. The COP is increasing with the increase in the outdoor temperature. For each outdoor

temperature, speeds of compressors and fans are adjusted via the variable speed drive. By adjusting the compressor speed, the condensation pressure is adapted to the heating demand. The COP increases when the condensation pressure decreases as shown in Figure 9.

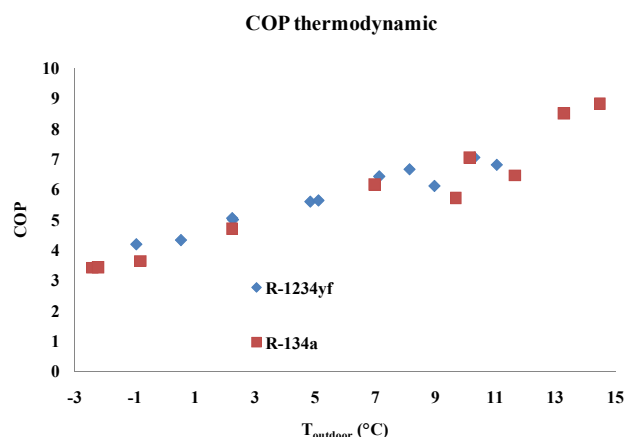


Figure 8: Variation of $COP_{thermodynamic}$ according to the outdoor temperature

Figure 9 shows also a comparison of R-134a and R-1234yf. R-1234yf presents a COP equal and sometimes higher than that of R-134a. This is due to the isentropic compression improvement with R-1234yf. Figure 10 shows the overall efficiency (Eq. 7) of compressors for two different refrigerants and for several compressor speeds.

$$\eta_{overall} = \frac{W_{isentropic}}{W_{electrical}} \quad (\text{Eq. 7})$$

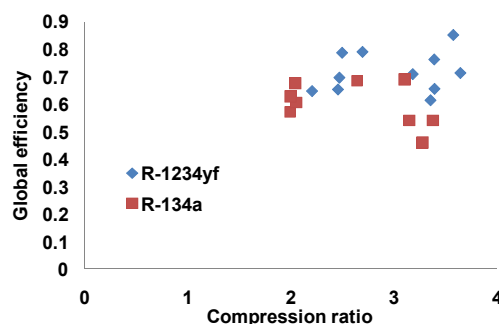


Figure 9: Variation of the compressor efficiency with the compression ratio

Figure 10 shows the variation of the COP_{system} . In fact, it decreases because of the fan consumptions especially for the low outdoor temperature.

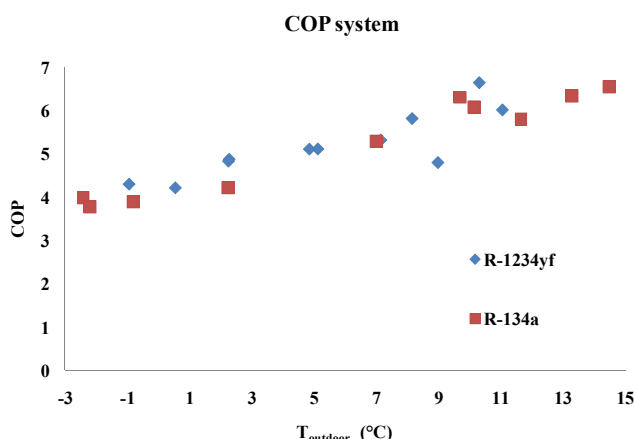


Figure 10: Variation of COP_{system} with the outdoor temperature

4.4 Internal heat exchanger (IHX)

The system was modified and an internal heat exchanger was added allowing heat exchange between the refrigerant in liquid phase leaving the condenser and the vapor at the evaporator exit. Figure 11 presents the variation of the $COP_{thermodynamic}$ for R-134a and R-1234yf. Effectively R-1234yf presents a COP higher than R-134a due to its thermodynamic properties.

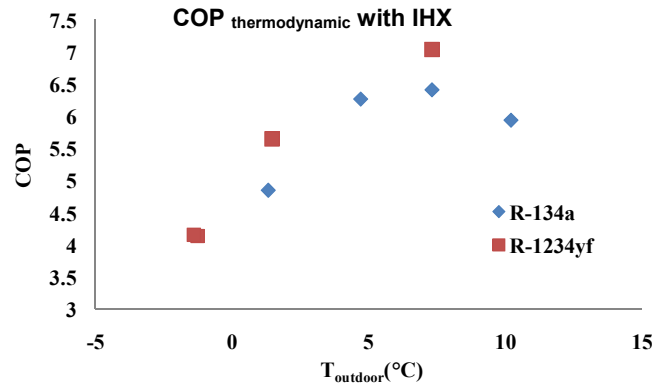


Figure 11: Variation of the $COP_{thermodynamic}$ with the outdoor temperature

4.5 Uncertainties

In order to calculate the COP uncertainties of the tests presented above, the method presented in Section 3 is used. For the air side, Equations 8 to 13 are combined to calculate the overall accuracy of the $Q_{Condenser}$ estimation.

$$Q_{condenser} = \dot{m}_{sup_plyair} (h_{out_air} - h_{in_air}) \quad (\text{Eq. 8})$$

$$\dot{m}_{air} = \rho_{air} \times \dot{V} \quad (\text{Eq. 9})$$

$$\rho_{air} = f(T, w) \quad (\text{Eq. 10})$$

$$w = f(T, RH, P_{sat}) \quad (\text{Eq. 11})$$

$$P_{sat} = f(T) \quad (\text{Eq. 12})$$

$$h = f(T, RH) \quad (\text{Eq. 13})$$

Equation 14 is used to calculate the heat recovered by the RHX.

$$Q_{RHX} = \dot{m}_{freshair} (h_{out_air} - h_{in_air}) \quad (\text{Eq. 14})$$

These equations and Equations 5 and 6 allow calculating the uncertainty on the COP estimation. Table 2 shows the higher uncertainties registered during tests.

Table 2: COP accuracy for different temperatures

Outdoor temperature (°C)	$\frac{UCOP_{thermod y n a m i c}}{COP_{thermod y n a m i c}} \%$	$\frac{UCOP_{system}}{COP_{system}} \%$
2.3	6.2	4.26
7.1	7.17	5.08
9.7	6.54	4.58
12.4	4.39	3.75

5 CONCLUSIONS

A new heating system is presented including an integrated recovery heat exchanger. The MHP presents a COP higher than 4 for an outdoor temperature of -3°C. The RHX ensures up to 35% of the heating demand of a low-energy building. Tests showed that R-1234yf presents a COP equal or higher than R-134a when using adapted components and control. The electrical consumption of fans affects significantly the COP.

The second version of this MHP can be improved by using other variable speed fans with lower electrical consumption.

6 REFERENCES

ASHRAE 2005. "ASHRAE Handbook-Fundamentals," Chapter 6: *Psychometrics*, American Society of Heating, Refrigerating, and Air-Conditioning Engineers, Inc., Atlanta.

Moffat R.J. 1988. "Describing the Uncertainties in Experimental Results", *Experimental Thermal and Fluid Science*, 1-3:17.

Mortada S., 2010. "Heat transfer performance of a mini-channel evaporator for heat pump application", Sustainable Refrigeration and Heat Pump Technology, KTH Stockholm, Sweden.

NF ENV 13005. 1999. Guide to the expression of uncertainty in measurement, AFNOR.

NOMENCLATURE

Q	capacity	W	Greek letters	
h	enthalpy	kJ.kg ⁻¹	ρ	density kg.m ⁻³
\dot{m}	mass flow rate	kg.s ⁻¹	ε	effectiveness
P _{sat}	pressure	bar	η	efficiency
RH	relative humidity	%	Subscripts	
T	temperature	K	CFA	complementary fresh air
U	uncertainty		COP	coefficient of performance
V	volumetric flow rate	m ³ .s ⁻¹	MHP	mini heat pump
w	absolute humidity	kg.kg ⁻¹	RHX	recovery heat exchanger
W	electric consumption	W		